Mayer-Gürr, T., Savcenko, R., Bosch, W., Daras, I., Flechtner, F., Dahle, C. (2012): Ocean tides from satellite altimetry and GRACE. - Journal of Geodynamics, 59-60, 28-38

DOI: 10.1016/j.jog.2011.10.009

Ocean tides from satellite altimetry and GRACE

Mayer-Gürr, T.[a], Savcenko, R.[b], W. Bosch[b], Daras, I.[c], Flechtner, F.[c], Dahle, Ch.[c]

[a] *Institute of Geodesy and Geoinformation, Bonn University, Bonn, Germany*
[b] *Deutsches Geodätisches Forschungsinstitut (DGFI), Munich, Germany*
[c] *GFZ German Research Centre for Geosciences, Potsdam, Germany*

Abstract

Satellite altimetry and GRACE observations carry both the signature of (residual) ocean tides and have in general complementary potential to resolve tidal constituents. It is therefore straightforward to perform a combined estimation of a global ocean tide model based on these two data sources. The present paper develops and applies a three step procedure for such a combined ocean tide model. First the processing of multi-mission altimetry data is described along with the harmonic analysis applied to derive initially a pure empirical ocean tide model. Then the capability of GRACE to sense particular tidal constituents is elaborated and an approach to estimate tidal constituents from GRACE is outlined. In a third step a combination strategy with optimal stochastic properties is developed and applied to the altimetry-only tide model EOT08a and four years of GRACE observations, leading to the combined model EOT08ag. The differential contributions of GRACE to EOT08ag remain small and are mainly concentrated to the Arctic Ocean, an area with little or poor altimetry data. In comparison with other tide models, EOT08ag is validated by K-band range residuals, the impact on gravity field modeling in terms of degree variances, precise orbit determination and variance reduction of crossover differences. None of these comparison exhibits a significant improvement over the altimetry-only tide model except for a few areas above 60°N. Overall the improvements of the combination remain small and appear to stay below the current GRACE baseline accuracy.

Keywords: Ocean tides, Satellite Altimetry, GRACE, EOT08ag

1. Introduction

Precise knowledge of ocean tides is indispensible for practical application like ship routing, the prediction of tidal heights and currents, the protection of the coastal ecosystem, for studying the dissipation of tidal energy, but also for the quantification of short-term mass variations in the Earth system, an application relevant in the context of the dedicated gravity field missions like GRACE and GOCE. The numerical treatment of ocean tides is based on Laplace shallow water equation as described for example by Hendershott (1977). Beside the gravitational forces of Moon and Sun, the land/ocean distribution and the sea floor topography must be taken into account to solve the differential equation. A challenge in the numerical treatment of tides is a proper accounting of dissipation, solid Earth effects, and modelling of baroclinic tides. Assimilating tidal constants from coastal or shallow water tide gauges have been performed to improve the accuracy of tidal prediction. A review on data assimilation may be found in Egbert and Bennett (1996).

In this paper we focus on pure empirical analysis of ocean tides as can be realized, for example, at an individual tide gauge by harmonic analysis of a sufficiently long record. On global scale the empirical analysis became feasible after satellite altimetry developed towards an operational technique and provided a few years time series of sea surface height measurements with a precision of a few centimetres (Mazzega, 1985). Consequently, after TOPEX completed a few years of operation, there was a great deal of new ocean tide models (Shum et al., 1997, 2001).

Since then, the altimeter observation scenario has been extremely improved. Today, there are nearly two decades of repeated sea level height measurements, performed over complementary ground track pattern of up to six different missions. There is significant progress in the precision of satellite ephemerides which are today exclusively based on GRACE gravity field models. The calibration of radiometer sensors has been improved as well as models used to correct for environmental effects (e.g. Scharroo et al., 2004). This altogether justifies a pure empirical approach, as demonstrated, for example, with the global ocean tide model EOT08a (Savcenko and Bosch, 2008). The comparison with other recent global ocean tide models demonstrate that the results of a pure empirical procedure are similar in performance as alternative approaches with or without assimilation (Ray et al., 2010).

However, some principle deficiencies of satellite altimetry remain: The sampling is not really global: above the latitude coverage of TOPEX, there are only GFO, suffering from a poor orbit determination, and the ESA missions ERS1/2 as well as ENVISAT, which fail to contribute to solar tides due to their sun-synchronous orbit configuration. Above all, the southern ocean has considerable large areas with seasonal sea ice coverage, making a reliable time series analysis nearly impossible.

Although alias problems for ocean tides are also present in

Email address: savcenko@dgfi.badw.de (Savcenko, R.)

the GRACE data (see section 3.1) it has been demonstrated that GRACE observation carries the signature of residual ocean tide signals for selected constituents (Knudsen, 2003; Bosch et al., 2009). A qualitative comparison of global ocean tide models by analysing the K-Band range data of GRACE was performed by Ray et al. (2009). Han et al. (2007) and Egbert et al. (2009) assimilate localized mass anomalies derived from GRACE ranging measurements into a hydrodynamic model to improve tidal solutions around Antarctica for the M2, S2, and O1 constituents. At the 2009 GRACE Science Team Meeting (Austin, Texas) a few presentations addressed again the potential to estimate ocean tides from time series of GRACE gravity fields. Han et al. (2010) point out that diurnal tides along the ascending and descending GRACE orbits are roughly opposite in phase and therefore mostly cancel in monthly gravity field solutions. They promote a separate treatment of ascending and descending tracks. Killett et al. (2009) solve for amplitudes and phases of major solar and lunar tides in the Arctic Ocean by inverting five years of GRACE inter-satellite acceleration data using the "mascon"-approach.

It is therefore self-evident to combine satellite altimetry and GRACE data for a common estimation of a global ocean tide model. The primary goal in this paper is to describe the procedure and first results for estimating a precise global ocean tide model by combining observations from GRACE and satellite altimetry in order to provide the most precise global description of the short-term tidal mass variations, a new ocean tide reference model for GRACE gravity field modelling, for satellite altimetry, and for studying the impact on Earth rotation, loading effects and other applications.

The present paper will first describe the processing of the altimeter data and the harmonic analysis performed for an altimetry-derived ocean tide model, EOT08a. In section 3 the tidal aliasing for the GRACE mission is explained, the sensitivity is investigated and the procedure is described, how individual tidal constituents can be estimated from GRACE observations. Then, section 4 outlines the approach to combine the altimetry-derived tide model with residual ocean tide signals derived from GRACE. The results of such a combination, the model EOT08ag, is introduced and validated by crossover statistics and analysis of GRACE range rate residuals. A final discussion and outlook reviews the combination procedure and indicates possible improvements for follow-on combined ocean tide modelling.

2. Altimetry data processing

2.1. Processing strategy and data pre-processing

Most of the classical pulse-limited radar altimeter systems provide sea surface height measurements along nominal ground track profiles, which are repeated after a fixed number of days. Sampling a high frequent ocean tide signal with dominant periods of 12 and 24 hours only every few days causes the well-known alias effects (see e.g. general discussion by Parke et al. (1987) and Smith (1999)): the high frequent signal becomes visible only after an alias period, much longer than the sampling period of the altimeter system. Sun-synchronous missions like ERS and ENVISAT pass the same location always at the same local time and cannot at all sense solar tides (they have an infinite alias period). In order to solve and mitigate the alias situation we take advantage of multi-mission altimetry with at least two, sometimes even five missions operating simultaneously with complementary ground track pattern. This multi-mission scenario exists since September 1992 (see Tab. 1).

Mission	Operation period [mm.yy]	Latitude coverage	Repeat cycle [days]	Ground track distance [km]
ERS-1	04.92 – 04.96	±81.5°	3/35/169	932/80/17
TOPEX	09.92 – 10.05	±66.1°	9.9156	315
ERS-2	04.95 – 04.03	±81.5°	35	80
GFO	01.00 – 09.08	±72.0°	17	165
Jason-1	01.02 – ...	±66.1°	9.9156	315
ENVISAT	09.02 – ...	±81.5°	35	80
ICESat	10.03 – 10.09	±86.0°	91	30
Jason-2	07.08 – ...	±66.1°	9.9156	315

Table 1: Satellite altimetry - mission overview with temporal and spatial sampling characteristics

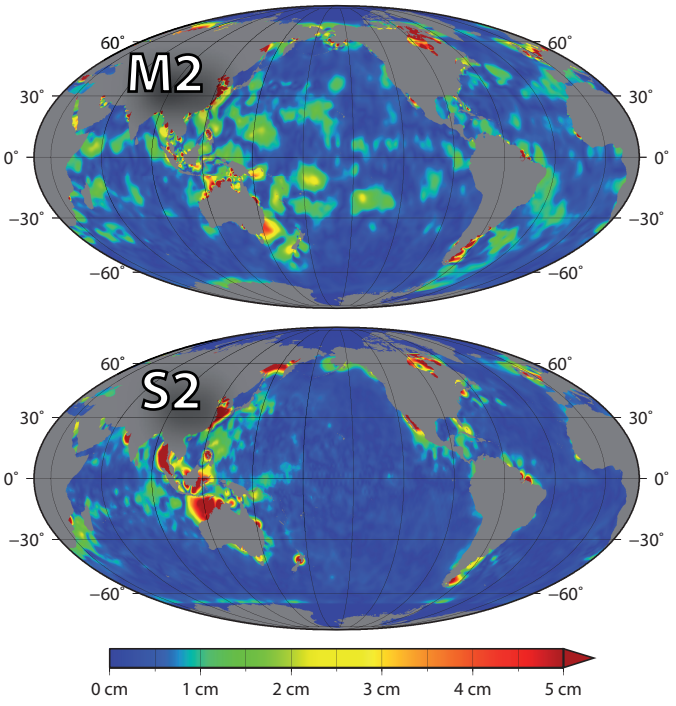

Figure 1: Residual tidal signal wrt. FES2004 of M2 and S2 (replacement grid)

The common ground track patterns of all altimeter satellites justify to perform – independent of the ground tracks of individual missions – the empirical analysis on a regular equidistant grid and to analyse all data inside a cap with spherical radius r_{max} around the grid nodes. This however is only possible if the data of all missions is updated, harmonized, and cross-calibrated. Updating implies to apply the most recent orbits and best known mission specific corrections, e.g. for the on

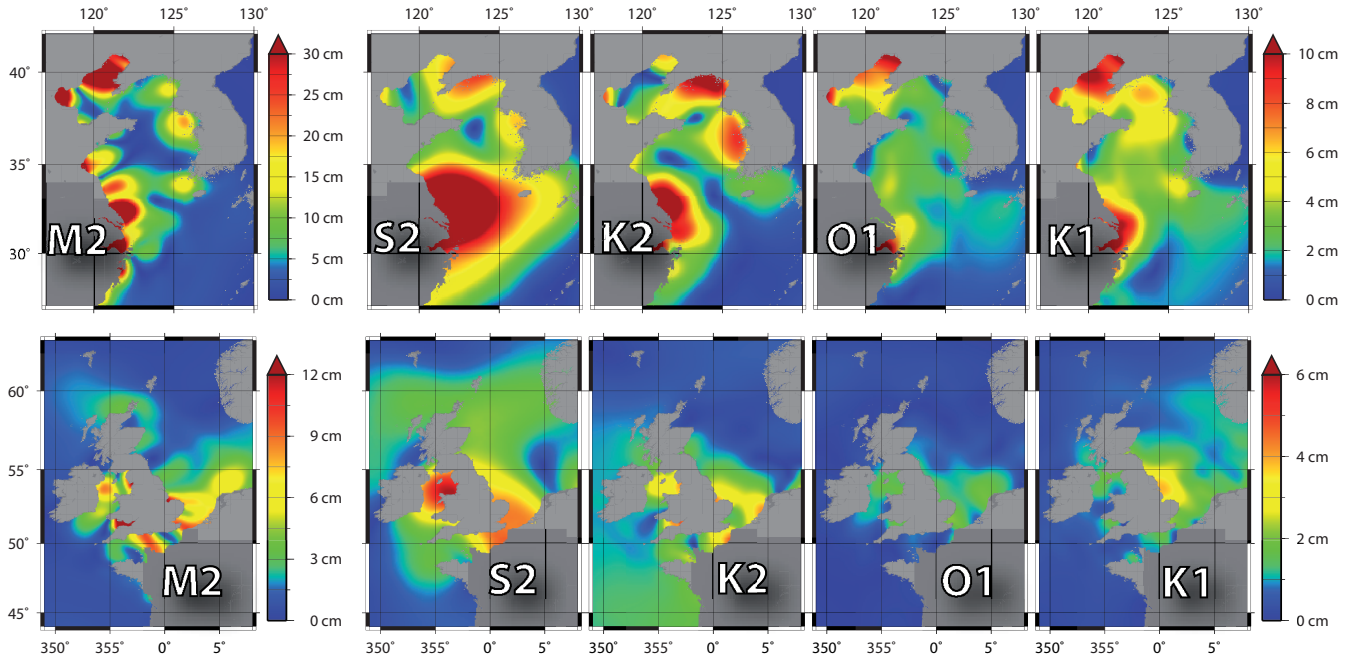

Figure 2: Residual tidal signal of EOT08a wrt. FES2004 of the some partial tides in Yellow Sea and on the North-West European Shelf

board microwave radiometers or the sea state biases. In addition, the data is harmonized by applying identical geophysical correction models e.g. for the inverted barometer effect, the reference tide model, and ionospheric prediction models for single frequency radar systems. Harmonization minimizes the risk to map systematic differences of correction models to the solve-for parameters of the ocean tide model. The cross-calibration is realized by means of a common least-squares analysis of cross-over differences performed between all altimeter systems operating simultaneously (Bosch and Savcenko, 2007). The estimated radial correction captures relative range biases and other geographically correlated errors. In summary, the laborious pre-processing results in widely consistent multi-mission data holdings, which justifies treating all observations as if they were taken by a single altimeter mission.

2.2. *Harmonic analysis of tidal constituents*

The data of all missions of Tab. 1 were pre-processed and de-tided by applying the ocean tide corrections derived from FES2004 (Lyard et al., 2006), a hydrodynamic model subsequently taken as reference. The harmonic analysis is then straight-forward and consists in estimating at every grid node residual tides from the sea surface heights h_k

$$\begin{aligned} h_k(t) + v_k = \; & m \\ + \; & \textstyle\sum_{i=1}^{n} f_i(t)\left[c_i \cos\left(\omega_i t + u_i(t)\right) + s_i \sin\left(\omega_i t + u_i(t)\right)\right] \\ + \; & \textstyle\sum_{j=1}^{m} \left[A_j \cos(\Omega_j t) + B_j \sin(\Omega_j t)\right] \end{aligned} \tag{1}$$

where v_k are residuals, m is a mean value and c_i and s_i are cosine and sine-coefficients to be solved for individual tidal constituents. The f_i and u_i are nodal corrections for amplitudes and phases of the astronomical arguments w_i respectively. In addition, cosine and sine-coefficients A_j and B_j for annual and semi-annual periods T_j with $\Omega_j = 2 \cdot \pi / T_j$ are solved for. The analysis is performed on every node of a 15'x15' geographical grid using cap sizes with $r_{max} = 1.5°$ in shallow water and $r_{max} = 4.5°$ in open ocean. The observations are weighted by a Gauss function taking its half weight width at $0.3 \cdot r_{max}$. The EOT08a solution solved for the constituents M2, S2, N2, K2, 2N2, O1, K1, P1, Q1, and M4. The residual amplitudes of the most dominant constituent M2 is shown in Fig. 1.

Shortly after the initial edition of EOT08a, a replacement of the "dynamic atmospheric correction (DAC[1])" for the ocean response to atmospheric pressure variations became available and led to significantly improved estimate of the residual S2 amplitudes (cf. Fig. 1). All investigations within this paper refer to the updated version of EOT08a.

In the meantime a modified solution, EOT10a, was also generated. EOT10a accounts for correlations among subsequent altimeter observation along the same pass and provides a more realistic error estimate. A variance-component estimate was applied to achieve a realistic relative weighting between the data from different missions. To rebut the suspicion that any tidal signal is mapped to the radial error estimates, the cross-calibration results were not applied for EOT10a. Instead a mission specific offset was estimated at each grid node. Correlation analyses (Savcenko and Bosch, 2008) showed that the tidal constituents are basically uncorrelated. This justified to perform

[1]Dynamic atmospheric Corrections are produced by CLS Space Oceanography Division using the Mog2D model from Legos and distributed by Aviso, with support from Cnes (*http://www.aviso.oceanobs.com/*)

	ST102 (96-102 TGs)				WOCE (158 TG)		
	EOT10a	EOT08a	FES2004	GOT4.7	EOT10a	EOT08a	FES2004
M2	**1.41**	1.44	1.45	1.46	11.85	12.06	**10.7**
S2	**0.84**	0.96	0.86	0.93	**4.20**	4.36	4.34
N2	**0.64**	0.65	0.67	**0.64**	2.53	2.66	**2.52**
K2	0.42	0.45	0.47	**0.40**	**1.51**	1.52	1.63
O1	**0.73**	0.74	0.75	0.76	2.98	**2.97**	3.02
K1	**0.96**	0.98	1.00	1.01	**4.02**	**4.02**	4.20
P1	**0.37**	0.42	0.40	**0.37**	**1.30**	1.32	1.37
Q1	0.28	0.30	0.30	**0.27**	0.68	**0.62**	0.68
M4					**1.23**	1.34	1.47

Table 2: RMS differences [cm] of tidal constants at tide gauges of the ST102p data set and of WOCE. Smallest values are indicated in bold

harmonic analyses for individual constituents with different cap sizes (r_{max} = 1.5°, 3°, 4.5°) homogeneously applied independent of water depth. EOT10a is a patchwork of tables from individual solutions selected according to the most favourite results of the validations described below. Compared to EOT08a, EOT10a provides additional tables for Mf, Mm, and S1.

2.3. Results and Validation

The residual amplitudes of EOT08a and EOT10a can hit significant magnitudes. For S2 and M2 the amplitude can take up to 15 cm over extended areas in shallow water like the North-West European shelf or the Yellow Sea (see Fig. 2). Residual amplitudes of the same magnitude are also found in the Indonesian Waters and on the Patagonian Shelf (both not shown here).

A widely used measure for the quality of global ocean tide models is the comparison with tidal constants. Tab. 2 compiles the RMS differences between global tide models and tidal constants of the ST102p set of tide gauges (Ray, private communication, 2007) and a set of WOCE sites (Ponchant and Lyard, 2008). For nearly all comparisons the empirical models GOT4.7 (Schrama and Ray, 1994; Ray, 1999), EOT08a, and EOT10a (this paper) show smaller RMS values than the hydrodynamic reference model FES2004 although some of the tide gauge data have been assimilated to FES2004 (Lyard et al., 2006).

For the ST102p tide gauges the EOT10a RMS values are always slightly lower than for EOT08a. The most significant improvements are achieved for the S2 constituent. However the comparisons at selected tide gauges are globally not absolutely representative. An exhaustive quality assessment requires much more comparisons. For the validation of EOT08a, statistics of crossover differences have been performed in addition (Savcenko and Bosch, 2008) and show for shallow water areas a significant gain in variance, if the residual tide correction of EOT08a were applied. Also the impact on GRACE range residuals have been studied for EOT08a (Bosch et al., 2009). As these comprehensive quality assessments for EOT10a are not yet fully completed, it was decided to use EOT08a with an updated table for the S2 constituent for the combination with GRACE.

3. GRACE data processing

3.1. Tidal aliasing

For the determination of ocean tides from GRACE data, it is necessary to investigate which of the tidal constituents can be estimated together with the monthly gravity field variations. Due to the orbit configuration GRACE does not permanently monitor every point of the ocean surface. This insufficient sampling rate results in mapping the high frequent tidal signal into lower frequencies (aliasing). In order to be able to separate the tides from the monthly variations, the aliasing periods of the tidal signal into the GRACE observations have to be shorter than one month.

As GRACE has no exact repeat orbit, it is not possible to calculate the aliasing frequencies of the different tidal constituents using closed formulas. Instead an analysis of the real GRACE orbits is required. Therefore, the over flights by GRACE during the time span from 2003 untill 2007 are compared to the oscillations of the major tides. In Fig. 3 the results are illustrated for a test area in the North Atlantic ($[20°W-35°W]\times[30°N-40°N]$). The tidal oscillations are indicated by the blue lines, the red dots mark the time when GRACE passes over this area.

The left part of Fig. 3 shows tidal constituents for 31 days with sub-monthly alias periods such as M2, O1, N2 and Q1. These constituents can be derived from GRACE data and will therefore be estimated together with the monthly gravity field variations in the following investigations. The right part of the figure illustrates constituents with aliasing periods longer than one month (shown for the full period of 2003-2007). Those constituents cannot be separated from monthly gravity field variations by GRACE. Therefore a common estimation together with the monthly gravity field variations is not possible. Other groups e.g. Han et al. (2007) pass on the monthly solutions and estimate also S2 but we think these monthly variations are one of the main purposes of the GRACE mission. Another reason is the strong sensitivity of GRACE to not modeled gravity field signals causing the well known striping patterns.

3.2. Sensitivity Analysis

If we would solve the full spectrum of all relevant constituents up to a certain degree and order (e.g. 20 or 30) the

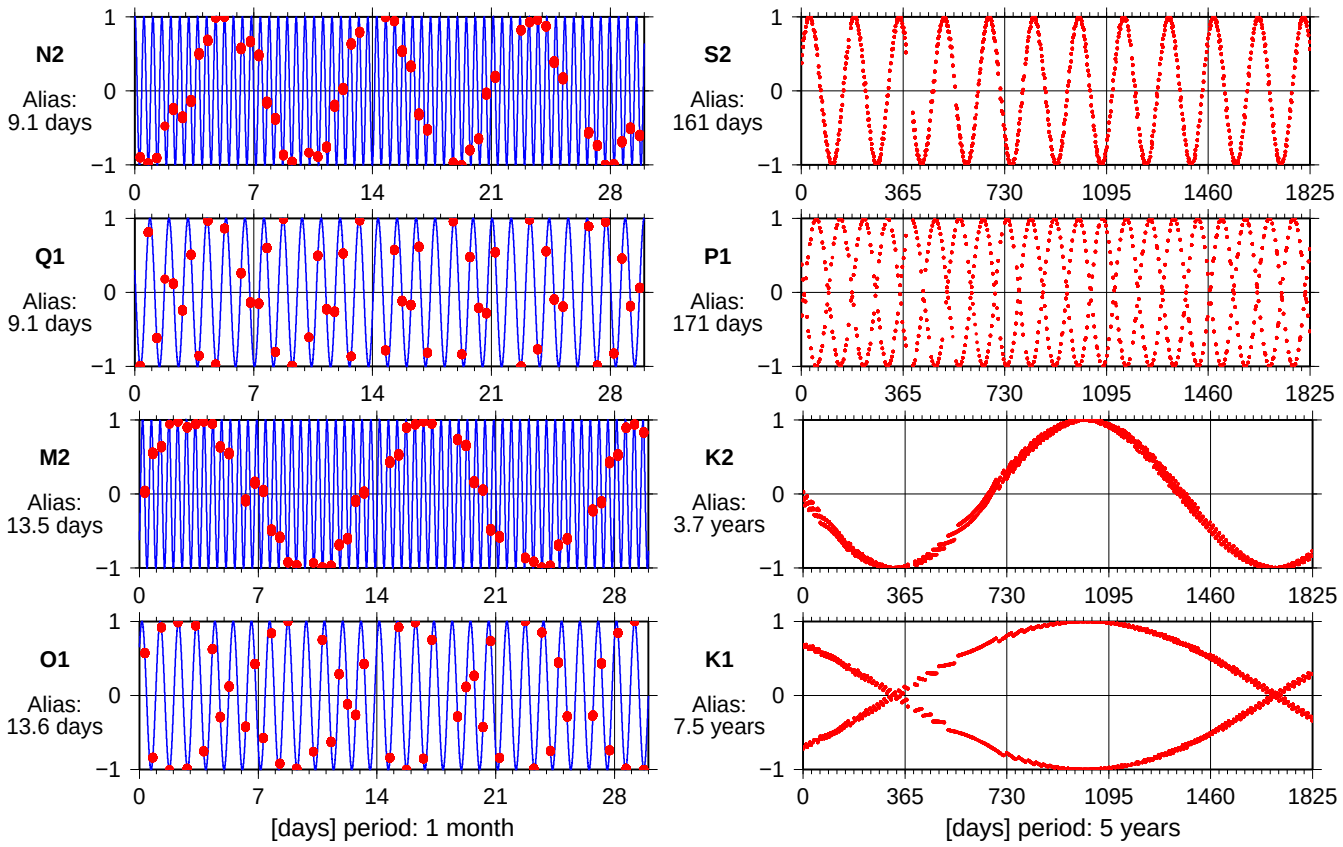

Figure 3: GRACE alias periods of different tidal constituents. The over flights by GRACE are compared to the oscillations of the major tides in a test area in the North Atlantic ($[20°W - 35°W] \times [30°N - 40°N]$). The partial tides can be separated into those featuring an alias period of less than one month (left) and those with a longer alias period (right).

number of additional parameters (besides the gravity field coefficients) would increase dramatically. Therefore, a sensitivity study based on the two ocean tide models FES2004 and EOT08ag has been performed in order to reduce the ocean tide unknowns to a reasonable smaller number.

The tide models are given in a spherical harmonic representation of amplitudes ($D^{\pm}_{lm,s}$) and phases ($\varepsilon^{\pm}_{lm,s}$), from which the coefficients $C^{\pm}_{lm,s}$, $S^{\pm}_{lm,s}$ can be retrieved by (Dow, 1988):

$$\begin{aligned} C^{\pm}_{lm,s} &= D^{\pm}_{lm,s} \cos \hat{\varepsilon}^{\pm}_{lm,s} = \tfrac{1}{2}(c_{lm,s} \pm b_{lm,s}) \\ S^{\pm}_{lm,s} &= D^{\pm}_{lm,s} \sin \hat{\varepsilon}^{\pm}_{lm,s} = \tfrac{1}{2}(a_{lm,s} \mp d_{lm,s}) \end{aligned} \tag{2}$$

where $\varepsilon^{\pm}_{lm,s} = \frac{\pi}{2} - \varepsilon^{\pm}_{lm,s} - \chi$ and $\chi = 0$ for a semidiurnal tides such as for M2.

The instantaneous ocean tide $\zeta_s(\lambda, \phi, t)$ can be expressed in terms of amplitude $\xi_s(\lambda, \phi)$ and phase lag $\delta_s(\lambda, \phi)$ as:

$$\zeta_s = \xi_s \cos(\theta_s + \chi_s - \delta_s) \tag{3}$$

where θ_s is the astronomical argument, χ_s depends on the tide (Dow, 1988). Eq. 3 can be expanded to:

$$\begin{aligned} \xi_s(\phi, \lambda) \cos \delta_s(\phi, \lambda) &= \sum_{l=0}^{\infty} \sum_{m=0}^{l} (a_{lm,s} \cos m\lambda \\ &\quad + b_{lm,s} \sin m\lambda)\, P_{lm}(\sin \phi) \\ \xi_s(\phi, \lambda) \sin \delta_s(\phi, \lambda) &= \sum_{l=0}^{\infty} \sum_{m=0}^{l} (c_{lm,s} \cos m\ \lambda \\ &\quad + d_{lm,s} \sin m\lambda)\, P_{lm}(\sin \phi). \end{aligned} \tag{4}$$

From Eq. 4 we solve for $a_{lm,s}$, $b_{lm,s}$, $c_{lm,s}$, $d_{lm,s}$ coefficients for both models. These coefficients are then used in Eq. 5 to compute the disturbing potential difference between the two ocean tide models at a near-GRACE orbital level of 500 km.

$$\begin{aligned} T_c &= 4\pi G R \rho_w \sum_{l=0}^{\infty} \left(\frac{R}{r}\right)^{l+1} \lambda' \sum_{m=0}^{l} (a_{lm,s} \cos m\lambda \\ &\quad + b_{lm,s} \sin m\lambda)\, P_{lm}(\sin \phi) \\ T_s &= 4\pi G R \rho_w \sum_{l=0}^{\infty} \left(\frac{R}{r}\right)^{l+1} \lambda' \sum_{m=0}^{l} (c_{lm,s} \cos m\lambda \\ &\quad + d_{lm,s} \sin m\lambda)\, P_{lm}(\sin \phi) \end{aligned} \tag{5}$$

where ϱ_w is the density of the sea water, $\lambda' = \frac{1+k_{l,s}}{2l+1}$, and $k_{l,s}$ are the load Love numbers.

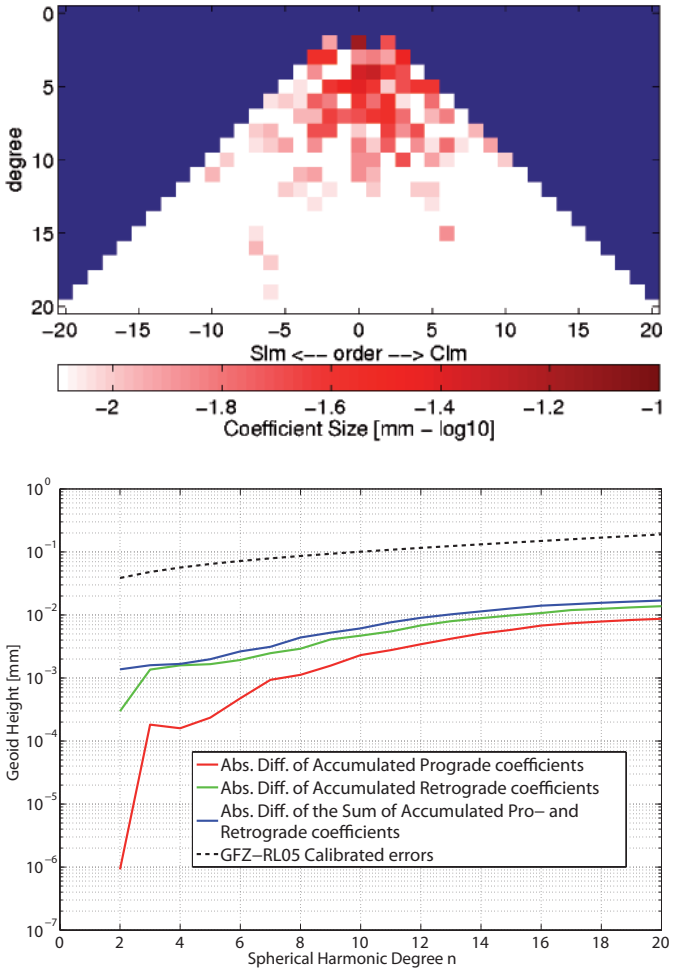

Figure 4: Sensitivity study result for M2 retro-grade and pro-grade amplitudes up to degree and order 20 with a threshold of 0.008 mm. Sensitive coefficients are marked in the red colour palette(top). Lower panel shows the accumulated "error" (difference between taking into account all or only sensitive coefficients) for accumulated prograde (red), retrograde (green) and sum of both coefficients (blue) as well as the current accumulated release 05 calibrated error (black) up to degree and order 20.

In the next step, a harmonic analysis of the disturbing potential difference with respect to the reference sphere of a radius equal to the semi-major axis of the Earth was performed, which resulted to the back tracing of the $a_{lm,s}$, $b_{lm,s}$, $c_{lm,s}$, $d_{lm,s}$ coefficients. From those coefficients the $C^{\pm}_{lm,s}$, $S^{\pm}_{lm,s}$ and finally the $D^{\pm}_{lm,s}$, $\varepsilon^{\pm}_{lm,s}$ are retrieved back, but this time representing the difference of the two models after the analysis.

Fig. 4 (top) shows the sensitivity study result for M2 retrograde and pro-grade amplitudes up to degree and order 20 with a threshold of 0.008 mm. Sensitive coefficients are marked in the red colour palette. This threshold value has a maximum impact of 0.009 mm for the accumulated pro-grade, 0.015 mm for the accumulated retro-grade coefficients and and 0.017 for the sum of both types of coefficients (Fig. 4 bottom) when taking into account all or only sensitive pro- and retrograde coefficients depicted in Fig. 4 (top). This maximum "error" is about a factor of 10 below the current release 05 GRACE error level of 0.2 cm (Flechtner et al., 2010) and can therefore safely be used to decrease the number of solved-for ocean tide coefficients. For M2, the number of sensitive coefficients could consequently be reduced from 436 to 100 or to 23%. Concerning the other tides, we determined the thresholds in such a way that the maximum impacts are close to the aforementioned levels for M2: a N2 threshold of 0.005 mm resulted in 57 sensitive coefficients (reduction to 13%) and a threshold of 0.004 mm for O1 resulted in 52 sensitive coefficients (reduction to 12%).

3.3. *Estimation of tidal constituents from GRACE data*

In the following, GRACE observations are used to improve existing ocean tide models. Here only those constituents with short aliasing periods are considered that were identified to be sensitive in the investigations of section 3.1. More than 4 years (09/2002 - 04/2007) of GRACE observations have been used in the calculations applying the same short arc approach and the same background models (astronomical tide of sun, moon and planets, Earth tides, atmospheric and ocean dealiasing product (AOD1B), ...) which have been used in the calculation of the ITG-Grace03s gravity field model, (Mayer-Gürr et al., 2010). As the ocean tide model FES2004 was applied as background model, the estimated constituents are the residuals to the FES2004 model.

The GRACE observations contain not only the residual ocean tide signals but all gravity field effects from other mass transports. GRACE is very sensitive to not modeled gravity field signals resulting in very noisy solutions. Therefore, monthly mean gravity field solutions have been co-estimated together with the ocean tide parameters in order to separate the ocean tide effect from other mass variations caused e.g. by hydrology. This is a new approach e.g. compared to Han et al. (2007). Thus it is reasonable not to include constituents with long aliasing periods into our analysis as, for example, S2 would be mapped completely into the monthly solutions and could not be distinguished from other gravitational effects.

For each month of GRACE data the observation equations can be formulated according to

$$l_G = A_G \delta x + \epsilon \quad \text{with} \quad \Sigma_{ll} = \sigma^2_G P^{-1}_G, \tag{6}$$

where l_G represents the GRACE K-band range observations reduced by the influence of the background models mentioned above. δx are the unkown parameters in terms of spherical harmonics and A_G stands for the functional model which establishes the relationship between observations and unknowns. The variance-covariance matrix of the observations Σ_{ll} is given by the inverse weight matrix P^{-1}_G multiplied by an unknown variance factor σ^2_G. The GRACE normal equations are then calculated by

$$n_G = N_G \delta x \quad \text{with} \quad N_G = A^T_G P_G A_G, \quad n_G = A^T_G P_G l_G. \tag{7}$$

From the monthly normal equations the monthly gravity field parameters will be eliminated, therefore in the following the δx contain only the residual ocean tide paramters. Afterwards all monthly normal equations of the given time span are accumulated to one complete system of normal equations.

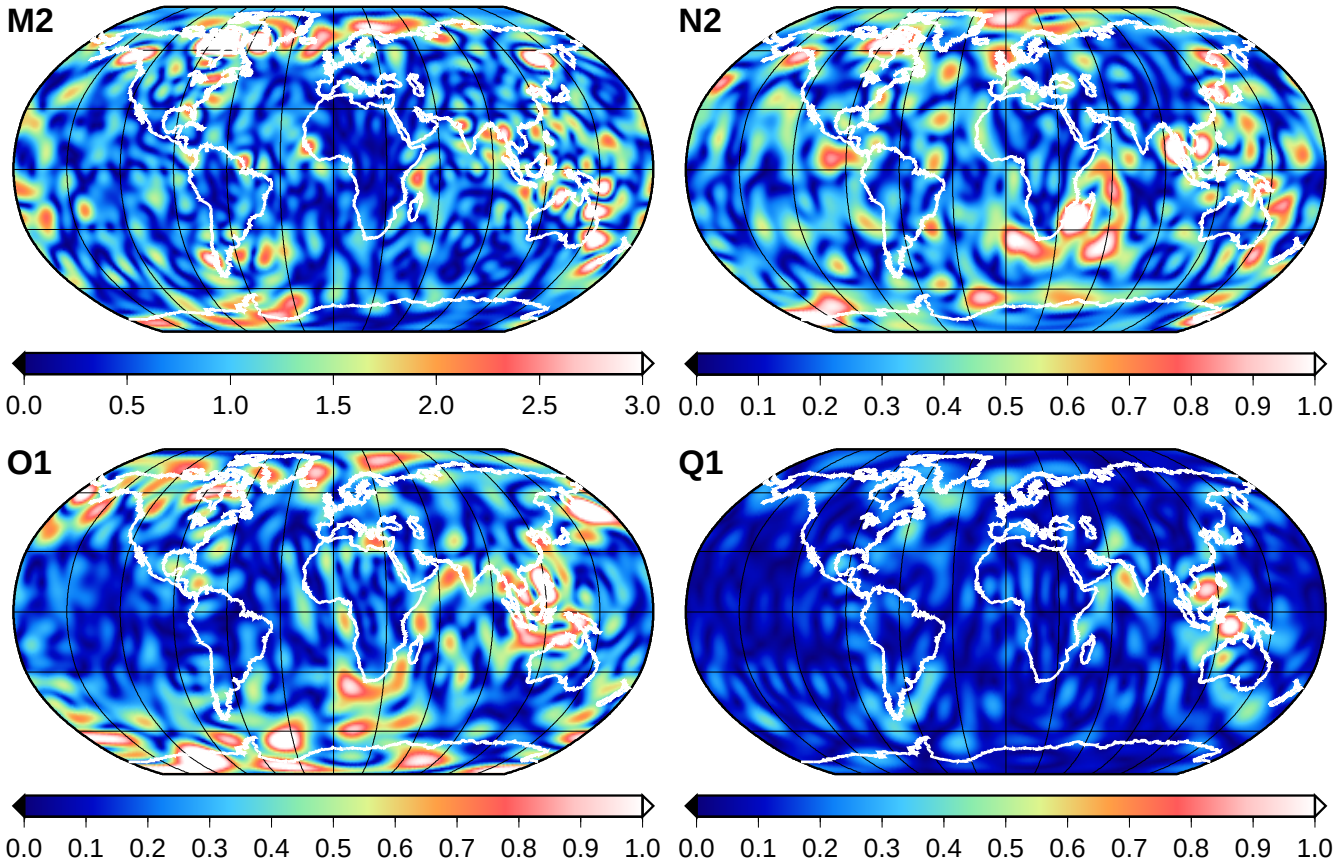

Figure 5: Residual amplitudes [cm] of different ocean tide constituents in cm as estimated from GRACE data compared to the FES2004 model.

The improvements are shown in terms of amplitudes of water heights in the Fig. 5 compared to the reference model FES2004. Large residual tidal signals can be observed in the coastal areas for each of the estimated constituents. Similar patterns can be identified when comparing the EOT08a model to the FES2004.

4. Combination strategy

As a next step, a combined empirical ocean tide model will be estimated using both GRACE and the given altimetry model introduced in Section 2. Altimetry models are customarily parameterized in terms of gridded values, whereas the GRACE solutions are given as spherical harmonic expansion. It was decided to carry out the combination on the basis of spherical harmonics, because it is expected that GRACE can only contribute to the larger spatial scales and it is thus possible to restrict the combination to these scales by limiting the spherical harmonic expansion to a moderate upper degree (see Section 3.2). The smaller scales are only taken from the gridded altimetry model as will be described below.

A stochastically optimal combination requires the knowledge of the respective covariance matrices. As this matrix has not yet been available in case of the altimetry model, an approximate model has to be derived. In a first approximation the gridded values of the EOT08a model are assumed to have equal variance and to be uncorrelated. As the model values are not directly used but transformed into a series of spherical harmonics the error behavior must be propagated to the Stokes coefficients. The transformation is performed according to

$$\begin{Bmatrix} c_{nm} \\ s_{nm} \end{Bmatrix} = \frac{\rho_w}{M} \frac{1+k'_n}{2n+1} \iint_\Omega \frac{r^{n+1}}{R^n} h(\lambda,\phi) \begin{Bmatrix} C_{nm}(\lambda,\phi) \\ S_{nm}(\lambda,\phi) \end{Bmatrix} d\Omega, \quad (8)$$

where h is the tidal height from the EOT08a model and ρ_w is the density of sea water. The Love numbers k'_n account for the potential of the loading deformation. Taking the property of orthogonality of the spherical harmonics into account the Stokes coefficients are also uncorrelated and their variances Σ are proportional to the following factor:

$$\Sigma \begin{Bmatrix} c_{nm} \\ s_{nm} \end{Bmatrix} \sim \left(\frac{1+k'_n}{2n+1} \right)^2 \quad (9)$$

This simple approximation also reveals that altimetry is less accurate in the lower degrees than it is in the higher degrees in terms of gravitational potential. In case of the GRACE solutions the situation is exactly opposite, here the lower degrees have higher accuracies than the higher degrees. This shows the potential of combining the two measurement techniques.

The altimetry model is introduced as pseudo-observations x_A in terms of spherical harmonics. The coefficients are reduced by the reference ocean tide model x_0 (FES2004) to be consistent with the GRACE processing model. This results in the

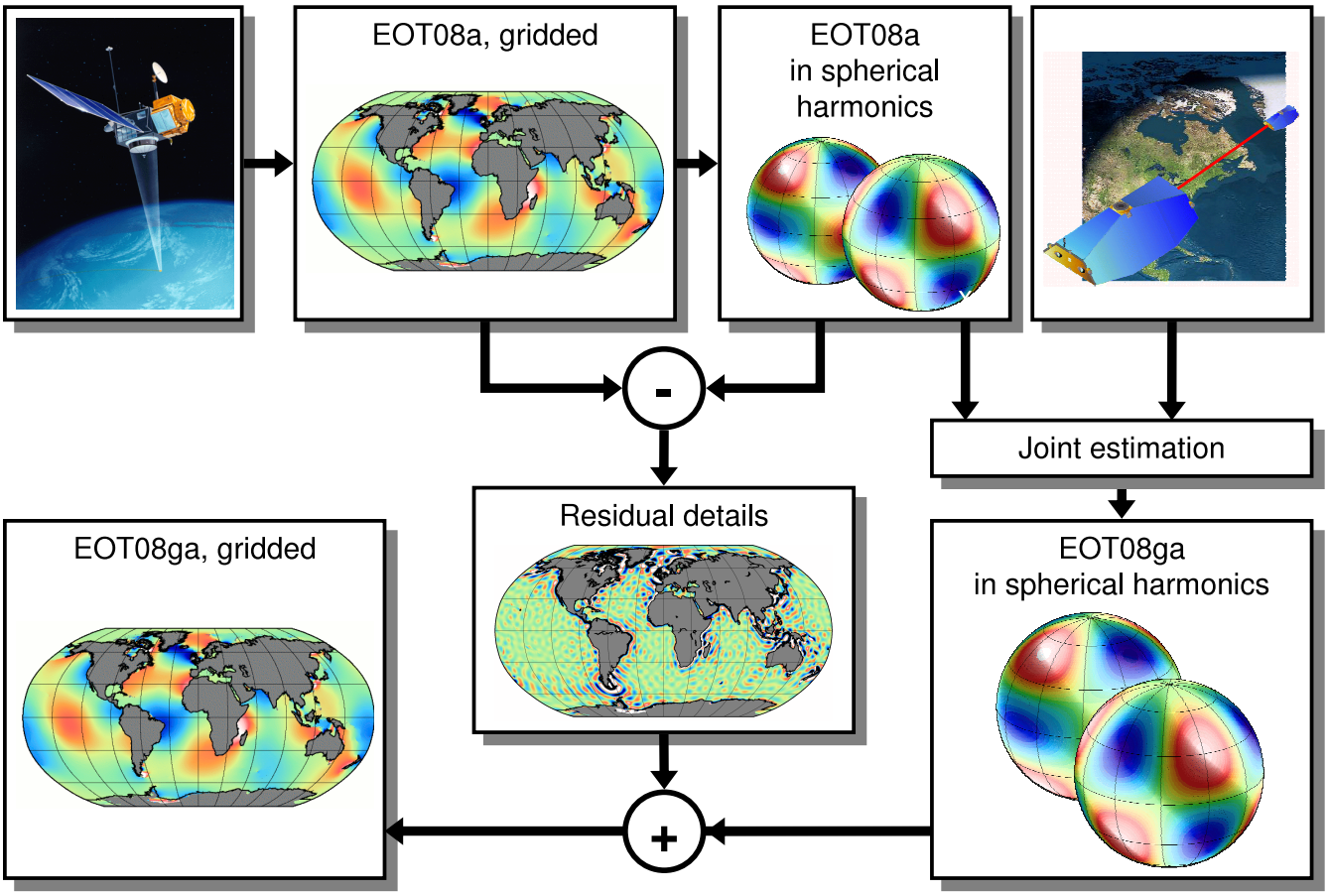

Figure 6: Combination schema of GRACE data and altimetry data.

following observation equations for the altimetric part

$$x_A - x_0 = I\delta x + \epsilon \quad \text{with} \quad \Sigma_{ll} = \sigma_A^2 P_A^{-1}. \tag{10}$$

The variance-covariance matrix is taken from (9). The combination of the GRACE observations and the altimetry pseudo observations results then in the following system of combined normal equations

$$\left(\frac{1}{\sigma_G^2} n_G + \frac{1}{\sigma_A^2} P_A (x_A - x_0)\right) = \left(\frac{1}{\sigma_G^2} N_G + \frac{1}{\sigma_A^2} P_A\right) \delta x \tag{11}$$

The relative weighting σ_A^2/σ_G^2 between the GRACE normal equations and the Altimeter normal equations are initialy unknown and estimated iteratively together with the combined solutions by means of variance component estimation (VCE, (Koch and Kusche, 2001)). From the combined model, gridded values can again be synthesized e.g. for oceanographic applications. As the combined model in terms of spherical harmonics only describes the large scales in the spatial domain, the missing detail structures must be taken from the gridded EOT08a model. These details are given as the difference between the original EOT08a model and the EOT08a model in terms of spherical harmonics evaluated at each grid point. Fig. 6 visualizes the different steps in the combination scheme.

The results of the combined analysis are displayed in Fig. 7. The plots show only the contribution of GRACE to the combined model in terms of amplitudes for different tidal constituents. Compared to the GRACE-only estimation (differences to FES2004) shown in Fig. 5, the signal is significantly smaller, which indicates the better agreement of GRACE with the EOT08a model. Furthermore the solution is smoother, as GRACE contributes less to the higher spatial resolution. Improvements can be observed especially in the polar regions, which appear to be reasonable as there is no data coverage by the altimetry satellites.

5. Validation

In order to validate the combined ocean tide modeling we investigated the influence of different background ocean tide models (FES2004, EOT08a, EOT08ag and EOT10a) on a monthly gravity field solution up to degree and order 120 for April 2008 using GFZs EPOS (Earth Parameter and Orbit System) software and the draft EIGEN-GRACE06S release 5 (RL05) processing standards and background models (update of RL04, Flechtner et al. (2010)). All tests were identical except that different ocean tide model were applied.

A first indication which of these four models is (absolutely) performing better is provided by the post-fit K-band Range Rate (KBRR) residuals which are calculated during the gravity field adjustment. Fig. 8 shows the daily RMS for all four cases. In

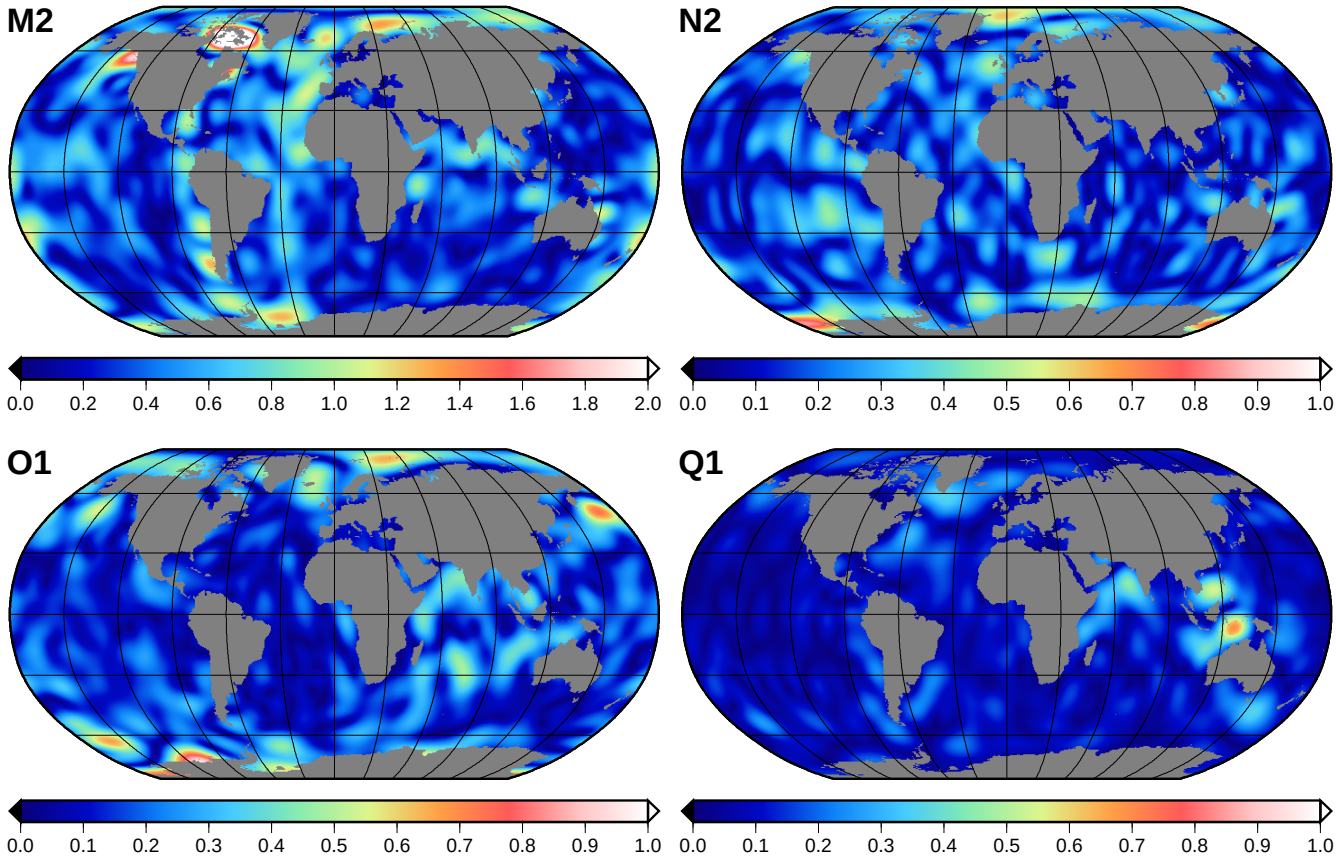

Figure 7: Amplitudes [cm] of the contribution of GRACE to the combined model

	RMS [mm]								
	GAUSS 500km			Unfilt. 120			Unfilt. 40		
	Global	Ocean	Land	Global	Ocean	Land	Global	Ocean	Land
FES2004	2.19	1.62	3.01	84.83	84.32	86.08	2.46	1.81	3.42
EOT08a	2.05	1.42	2.93	84.30	83.91	85.27	2.34	1.63	3.36
EOT08ag	2.05	1.42	2.93	83.35	83.00	84.25	2.34	1.62	3.35

Table 3: RMS values of geoid heights for a monthly gravity field using different models. Results are shown for the solution after applying the Gaussian 500km filter, for the unfiltered solution up to degree and order 120 and for the unfiltered solution truncated at degree 40.

principle all KBRR residual curves are very close to each other, but the combined EOT08ag model has slightly smaller residuals (especially for arcs 15 - 20) than the others. Also, the results for sub-daily (regional) comparisons may look different and have to be investigated.

We found that the global impact of changing the background ocean tide models in a monthly gravity field is of minor importance. The formal geoid errors of the monthly solutions are almost the same in each case and their degree variance differences are also very close (Fig. 9) and still below the draft GFZ RL05 calibrated GRACE error level (factor of 11 above the GRACE baseline). In particular, the degree variance difference between the field using the EOT08ag and the field using the EOT08a model is in the level of the baseline of GRACE, which means that the impact of GRACE to the combination with the altimetry model is presently on the noise level and cannot be sensed by the monthly gravity field estimation. As for the KBRR residuals, the regional impact may be more significant and has to be further investigated.

The indication from the KBRR test, that the combined EOT08ag model improves monthly gravity field solutions, is more encouraged by the results in Tab. 3. Here, the RMS of geoid heights of monthly gravity fields derived from different ocean tide models and filters are shown. Both EOT models improve the FES results over the oceans by about 12% in case a Gauss filter is applied. The unfiltered results, which show the internal quality of a monthly solution, also improve by 10% for n_{max} = 40 (500km) with an additional gain of 1% when using EOT08ag.

The four ocean tide models have also been tested in the precise orbit determination (POD) of various geodetic satellites and various observation types (SLR, PRARE, Doris). The re-

Satellite	Observation Type	#arcs	#arc length [d]	FES2004	EOT08a	EOT08ag	EOT10a
GFZ-1	SLR	5	3	13.78	13.77	13.77	13.76
STELLA	SLR	5	3	2.93	2.92	2.91	2.89
STARLETTE	SLR	5	3	2.52	2.52	2.51	2.53
AJISAI	SLR	5	3	3.18	3.17	3.17	3.16
LAGEOS-1	SLR	3	6	1.03	1.03	1.03	1.03
LAGEOS-2	SLR	3	6	1.03	1.04	1.04	1.03
ERS-2	SLR	6	6	5.32	5.29	5.29	5.29
ERS-2	PRA	6	6	3.57	3.58	3.58	3.56
ERS-2	PDO	6	6	0.346	0.346	0.345	0.345
ENVISAT	SLR	7	4-8	4.44	4.33	4.35	4.63
ENVISAT	DOR	7	4-8	0.496	0.496	0.496	0.496
WESTPAC	SLR	5	6	4.09	4.09	4.09	4.07
JASON-1	SLR	6	10	1.83	1.84	1.84	1.83

Table 4: SLR [cm], PRARE Range (PRA [cm]), PRARE Doppler (PDO) [mm/s] and Doris (DOR) [mm/s] RMS values for various geodetic satellites and observation types

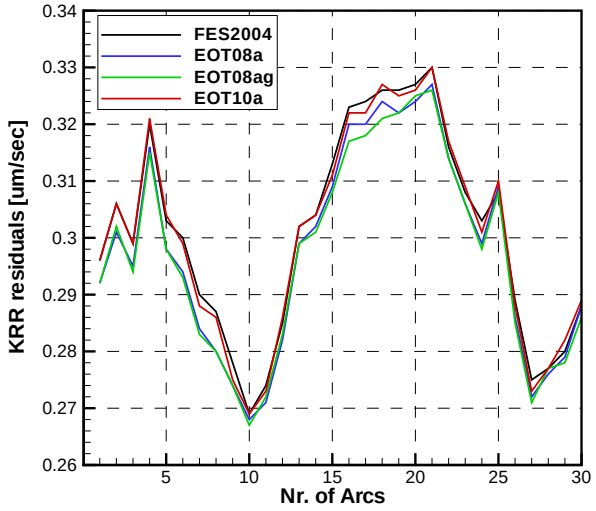

Figure 8: Daily post-fit K-band Range rate (KRR) residuals (μm/s) for fields using all the different models.

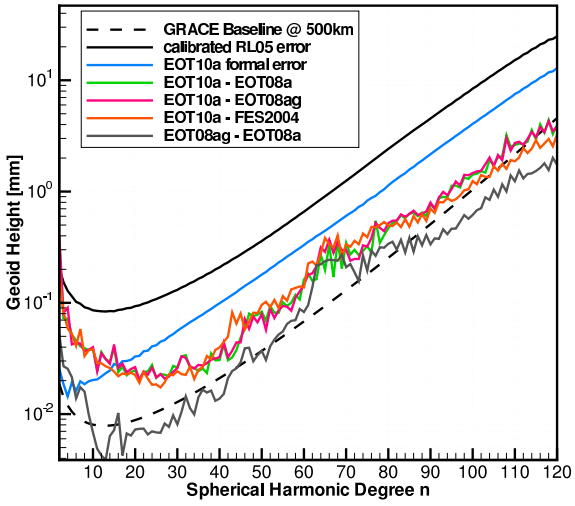

Figure 9: Degree variance differences of monthly gravity field using different background ocean tide models as well as the formal error of the gravity field using EOT10a

sults (see Tab. 4) show that generally a) FES2004 provides the largest RMS values, b) EOT08ag is slightly better than EOT08a and c) EOT10 gives smallest RMS values.

Finally, the performance of the gridded form of the combined EOT08ag model (c.f. the lower left square in Fig. 6) is validated by a statistical comparison of crossover differences. The sea surface heights observed by altimetry at different epochs are to be corrected for ocean tides in order to be comparable. Consequently, any ocean tide model causing smaller variances for the discrepancies between the corrected sea surface heights at the crossing of ascending and descending tracks is supposed to explain the temporal variations better than any other model. Therefore the variance of crossover differences have been compared between a processing using EOT08a as ocean tide correction and an alternative processing using EOT08ag. The variance reduction, if EOT08a is replaced by EOT08ag, is shown in Fig. 10. The red color indicates a variance reduction, while blue exhibits an increase of variances. In open ocean there is no clear indication, except for a few areas above 60° N. In particular ENVISAT and GFO show a significant variance reduction of about 5 cm^2 in the Arctic Ocean. Thus at least at the northern latitude the combined model EOT08ag performes better than the altimetry-only model EOT08a.

6. Summary and Outlook

The present investigation aimed to estimate a global ocean tide model by combining empirical results obtained from satellite altimetry with global analysis of GRACE data. For the

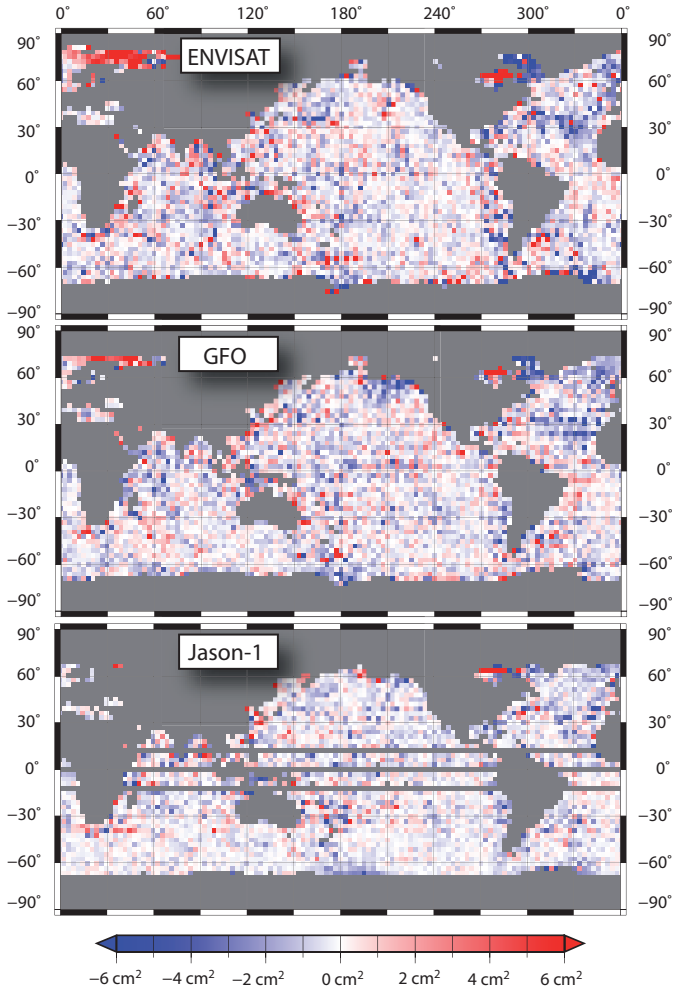

Figure 10: Variance reduction of crossover differences for ENVISAT, GFO, and Jason-1 if the EOT08a tide corrections for the sea surface heights are replaced by the tide correction of the combined model EOT08ag. The red color indicates a reduction, while blue exhibits an increase of variances. The large ground track spacing of Jason-1 causes three empty 3°-wide latitude circles without any crossover points. For ENVISAT and GFO there is an increase of variances in the North Atlantic which may be explained by a mission specific alias effect of unresolved water mass variations.

analysis of GRACE data the set of tidal constituents was co-estimated with monthly gravity fields. This implies that high frequent tidal signals are mapped into lower frequencies of the gravity field (aliasing). In order to separate the tides from the monthly gravity variations, the aliasing periods of the tidal signal have to be shorter than one month and only tides such as M2, O1, N2 or Q1 can be adjusted from GRACE. In principle is is possible to estimate further tidal constituents but in this case it is impossible to co-estimate monthly gravity field variations, one of the main products of the GRACE mission. In order to reduce the number of tidal spherical harmonic coefficients which have to be solved in parallel to the gravity spherical harmonic coefficients we have performed a sensitivity analysis and showed that we can reduce the number of additional tidal unknowns to approximately 20%. The resulting GRACE normal equation systems have been used to derive residual signals for four tidal constituent with respect to FES2004, namely M2, O1, N2, and Q1. A statistically optimal combination of GRACE and altimetry (EOT08a) has been developed and applied using a-priori covariance matrices resulting in the EOT08ag model. This model shows slight improvements compared to the altimetry-only model EOT08a when looking at K-Band range-rate or SLR residuals during POD of various geodetic satellites. Unfortunately the benefit of the new EOT models for a global monthly gravity field solution is not yet visible. Therefore we will change our strategy in the future from global spherical harmonics to tailored localized base functions in order to take advantage of the good global coverage of GRACE in Polar Regions where altimetry is still of poor quality.

Acknowlegements

This work was funded by the Deutsche Forschungsgemeinschaft (DFG), Bonn, Germany, under the grants BO1228/5-2, FL592/2-2, and *IL 17/9-1*

We would like to thank the German Space Operations Center (GSOC) of the German Aerospace Center (DLR) for providing continuously and nearly 100% of the raw telemetry data of the twin GRACE satellites.

References

Bosch, W. and R. Savcenko (2007). Satellite altimetry – multi-mission cross calibration. In C. Rizos (Ed.), *Dynamic Planet – Monitoring Understanding a Dynamic Planet with Geodetic Oceanographic Tools*, Volume 130 of *IAG Symposia*, pp. 51–56. Springer.

Bosch, W., R. Savcenko, F. Flechtner, C. Dahle, T. Mayer-Gürr, D. Stammer, E. Taguchi, and K.-H. Ilk (2009). Residual ocean tide signals from satellite altimetry, grace gravity fields, and hydrodynamic modelling. *Geophys. J. Int. 178*, 1185–1192.

Dow, J. (1988). Ocean tides and tectonic plate motions from lageos. *Deutsche Geodätische Komission, Reihe C, Heft Nr. 344, München*.

Egbert, G. D. and A. F. Bennett (1996). Data assimilation methods for ocean tides. In P. Malonotte-Rizzoli (Ed.), *Modern Approaches to Data Assimilation in Ocean Modeling*, pp. 147–179. Elsevier Science.

Egbert, G. D., S. Y. Erofeeva, S.-C. Han, S. B. Luthcke, and R. D. Ray (2009). Assimilation of grace tide solutions into a numerical hydrodynamic inverse model. *Geophys. Res. Lett.* (36), L20609.

Flechtner, F., C. Dahle, K. Neumayer, R. König, and C. Förste (2010). The release 04 champ and grace eigen gravity models. In F. Flechtner, M. Mandea, T. Gruber, M. Rothacher, J. Wickert, and A. Güntner (Eds.), *System Earth via Geodetic-Geophysical Space Techniques, Adv. Technologies in Earth Sciences*. Springer-Verlag Berlin Heidelberg.

Han, S.-C., R. D. Ray, and S. B. Luthcke (2007). Ocean tidal solution in antarktica from grace intersatellite tracking data. *Geophys. Res. Lett.* (34), L21607.

Han, S.-C., R. D. Ray, and S. B. Luthcke (2010). One centimeter-level observations of global diurnal ocean tides from monthly mean time-variable gravity fields. *Journal of Geodesy* (84), 715–729.

Hendershott, M. C. (1977). Numerical models of ocean tides. In E. D. Goldberg (Ed.), *The Sea. Vol. 6: Marine Modeling*, pp. 47–96. Wiley.

Killett, B., J. Wahr, S. Desai, D.-N. Yuan, and M. Watkins (2009). Arctic ocean tides from grace satellite accelerations. In *Proceedings of the GRACE Science Team Meeting*, pp. 641. Centre of Space Research.

Knudsen, P. (2003). Ocean tides in grace monthly averaged gravity fields. *Sp. Sci. Rev. 108*(1), 261–270.

Koch, K. R. and J. Kusche (2001). Regularization of geopotential determination from satellite data by variance components. *Journal of Geodesy 76*(5), 641–652.

Lyard, F., F. Lefevre, T. Letellier, and O. Francis (2006). Modelling the global ocean tides: modern insights from FES2004. *Ocean Dynamics* (56), 394–415.

Mayer-Gürr, T., A. Eicker, E. Kurtenbach, and K.-H. Ilk (2010). ITG-GRACE: Global static and temporal gravity field models from GRACE data. In F. Flechtner, T. Gruber, A. Güntner, M. Mandea, M. Rothacher, T. Schöne, and J. Wickert (Eds.), *System Earth via Geodetic-Geophysical Space Techniques*. Springer.

Mazzega, P. (1985). M2 model of the global ocean tide derived from SEASAT altimetry. *Mar. Geod. 9(3)*, 335–363.

Parke, M., R. Stewart, and D. Farless (1987). On choice of orbit for an altimetric satellite to study ocean circulation and tides. *J. Geophys. Res. 92(C11)*, 11,693–11,707.

Ponchant, F. and F. Lyard (2008). Tidal constants. World Ocean Circulation Experiment (woce) sea level Data Assembly Centre (DAC). Website. *www.bodc.ac.uk/projects/international/woce/tidal_constants/*; downloaded in 2008.

Ray, R. D. (1999). A global ocean tide model from topex/poseidon altimetry: Got99.2. Technical report, Goddard Space Flight Center, NASA/TM-1999-209478, pp58.

Ray, R. D., G. D. Egber, and S. Y. Erofeeva (2010). Tide predictions in shelf coastal waters: status prospects. In S. Vignudelli, A. G. Kostianoy, P. Cipollini, and J. Benveniste (Eds.), *Coastal Altimetry*. Springer-Verlag.

Ray, R. D., S. B. Luthcke, and J.-P. Boy (2009). Qualitative comparisons of global ocean tide models by analysis of intersatellite ranging data. *J. Geophys. Res.* (114), C09017.

Savcenko, R. and W. Bosch (2008). Eot08a - empirical ocean tide model from multi-mission satellite altimetry. Technical Report 81, Deutsches Geodätisches Forschungsinstitut, München, Germany.

Scharroo, R., J. L. Lillibridge, W. H. F. Smith, and E. J. O. Schrama (2004). Cross-calibration and long-term monitoring of the microwave radiometers of ERS, TOPEX, GFO, Jason, and ENVISAT. *Mar. Geod. 27*(1), 279–297.

Schrama, E. and R. Ray (1994). A preliminary tidal analysis of TOPEX/Poseidon altimetry. *J. Geophys. Res. 99(C12)*, 24,799–24,808.

Shum, C., N. Yu, and C. Morris (2001). Recent advances in ocean tidal science. *J. Geodetic Society of Japan 47(1)*, 528–537.

Shum, C. K., P. L. Woodworth, O. B. Andersen, G. D. Egbert, O. Francis, C. King, S. M. Klosko, C. L. Provost, X. Li, J.-M. Molines, M. E. Parke, R. D. Ray, M. G. Schlax, D. Stammer, C. C. Tierney, P. Vincent, and C. I. Wunsch (1997). Accuracy assessment of recent ocean tide models. *J. Geophys. Res. 102(C11)*(25), 25,173–25,194.

Smith, A. (1999). *Application of satellite altimetry for global ocean tide modelling.* Ph. D. thesis, Institute for Earth-Oriented Space Research. Delft University of technology. Faculty of Aerospace Engineering.